

Cherenkov radiation in coupled long Josephson junctions

E. Goldobin,* A. Wallraff,† N. Thyssen, and A. V. Ustinov†

Institute of Thin Film and Ion Technology, Forschungszentrum Jülich GmbH (KFA), D-52425 Jülich, Germany

(Received 22 August 1997)

Evidence for Cherenkov radiation of a Josephson vortex is observed in the system of two magnetically coupled long Josephson junctions. This radiation leads to resonances which appear above the lowest characteristic velocity \bar{c}_- of the linear electromagnetic waves. Resonances result from interaction of a Cherenkov wave with a moving Josephson vortex and, in annular junctions, occur when the vortex makes one turn around the junction. Experimental data are in good agreement with the proposed model and simulations which provide a clear physical picture of the observed effect. [S0163-1829(97)01046-1]

Cherenkov radiation exists if a particle moves with the velocity equal to the phase velocity of the emitted waves. Electromagnetic waves in a long Josephson junction (LJJ) are described by the sine-Gordon equation which has, in particular, soliton (Josephson vortex) and linear wave (Josephson plasma) solutions. A soliton behaves as a quasiparticle with its own characteristic mass and velocity. The highest possible velocity of the soliton, \bar{c}_0 , coincides with the lowest phase velocity, the Swihart velocity, of linear electromagnetic waves. Therefore Cherenkov radiation does not appear in conventional LJJ's.

Recently, there has been a growing interest in mutually coupled LJJ systems¹⁻⁶ described by coupled sine-Gordon equations. Such structures are typically stacks of Josephson junctions that either can be prepared artificially using well established Nb-Al-AIO_x-Nb technology^{2,5} or appear naturally in layered high- T_c superconductors that exhibit intrinsic Josephson effect.⁴ Since the dispersion relation for linear waves as well as the maximum velocity of a vortex are influenced by mutual coupling of the junctions,^{5,6} one may ask if Cherenkov radiation can appear in coupled LJJ systems.

In the simplest system of two stacked LJJ's the minimum phase velocity of linear waves depends on the propagation mode and is equal to $\bar{c}_\pm = \bar{c}_0 / \sqrt{1 \pm S}$, where $+$ holds for the in-phase mode and $-$ for the out-of-phase mode; S ($-1 < S < 0$) is a dimensionless coupling constant.⁵ When discussing different soliton configurations we use the notation $[N|M]$ throughout this paper, which means N solitons located in one LJJ and M solitons in the other LJJ ($N, M < 0$ describe antisolitons). The maximum velocity of the (anti-)symmetric soliton states in the coupled LJJ system is equal to \bar{c}_+ for the in-phase $[1|1]$ and \bar{c}_- for the out-of-phase $[1|-1]$ soliton mode. For such symmetric and antisymmetric modes the system of two coupled sine-Gordon equations splits into two independent sine-Gordon equations. This, again, results in a coincidence of the maximum velocity of the soliton with the lowest phase velocity of the linear waves and, thus, the absence of Cherenkov radiation.

The asymmetric $[1|0]$ soliton mode received little attention until now and even the question about the maximum velocity of a soliton in this mode remains open. In this paper we report the experimental and numerical study of single soliton dynamics in the $[1|0]$ state.

In order to investigate the influence of coupling on the soliton dynamics, we have chosen the most ideal ring-shape (annular) junction geometry.^{7,8} Due to magnetic-flux quantization in a superconducting ring, the number of vortices initially trapped in an annular junction is conserved. The soliton dynamics can be studied here under periodic boundary conditions which exclude a complicated interference of the soliton with the junction edges.

Experiments have been performed with (Nb-Al-AIO_x)₂-Nb annular LJJ. The mean diameter of all LJJ's was $D = 132 \mu\text{m}$ and the width $W = 10 \mu\text{m}$. A typical normalized circumference of the ring was $\pi D / \lambda_J = L / \lambda_J \approx 7$, where λ_J is the Josephson penetration depth. Vortex trapping was realized by applying a small bias current to the junction while cooling the sample below the critical temperature $T_c^{\text{Nb}} = 9.2 \text{K}$. Measurements were performed at 4.2 K.

Before presenting the experimental results obtained for two coupled LJJ's, in Fig. 1(a) we show the single-soliton current-voltage characteristic (IVC) of a single annular LJJ of the same dimensions. The bias current I creates a Lorentz force which drives the soliton; the measured dc voltage V is proportional to the soliton velocity. With increasing I , the velocity of the Josephson vortex increases, and rather quickly reaches the relativistic region which accounts for the step with the asymptotic voltage $V_1 \approx 52 \mu\text{V}$ in Fig. 1(a). This voltage yields the Swihart velocity $\bar{c}_0 \approx V_1 \pi D / \Phi_0 \approx 0.035c$, where Φ_0 is the magnetic-flux quantum, and c is velocity of light in vacuum.

In stacked annular LJJ's, trapping of a single vortex was more difficult due to the asymmetry of the required state $[1|0]$. Therefore, after every trapping attempt, the resulting state was carefully checked by several means. First, the IVC of the system was traced. A large critical current I_c implies the $[0|0]$ configuration. If I_c is close to zero, the voltage of a soliton step on IVC has to be proportional to the total number of vortices trapped in the system minus the number of pinned vortices. Second, the dependences of the critical current I_c and the maximum current at the single junction gap voltage I_g on magnetic field H applied in the plane of the sample were measured. The soliton configuration was deduced from the shape of $I_c(H)$ and $I_g(H)$.⁹ As shown in Fig. 1(c), in the $[1|0]$ state $I_c(H)$ has a minimum at $H = 0$ and $I_g(H)$ has a maximum. The LJJ in the stacks under

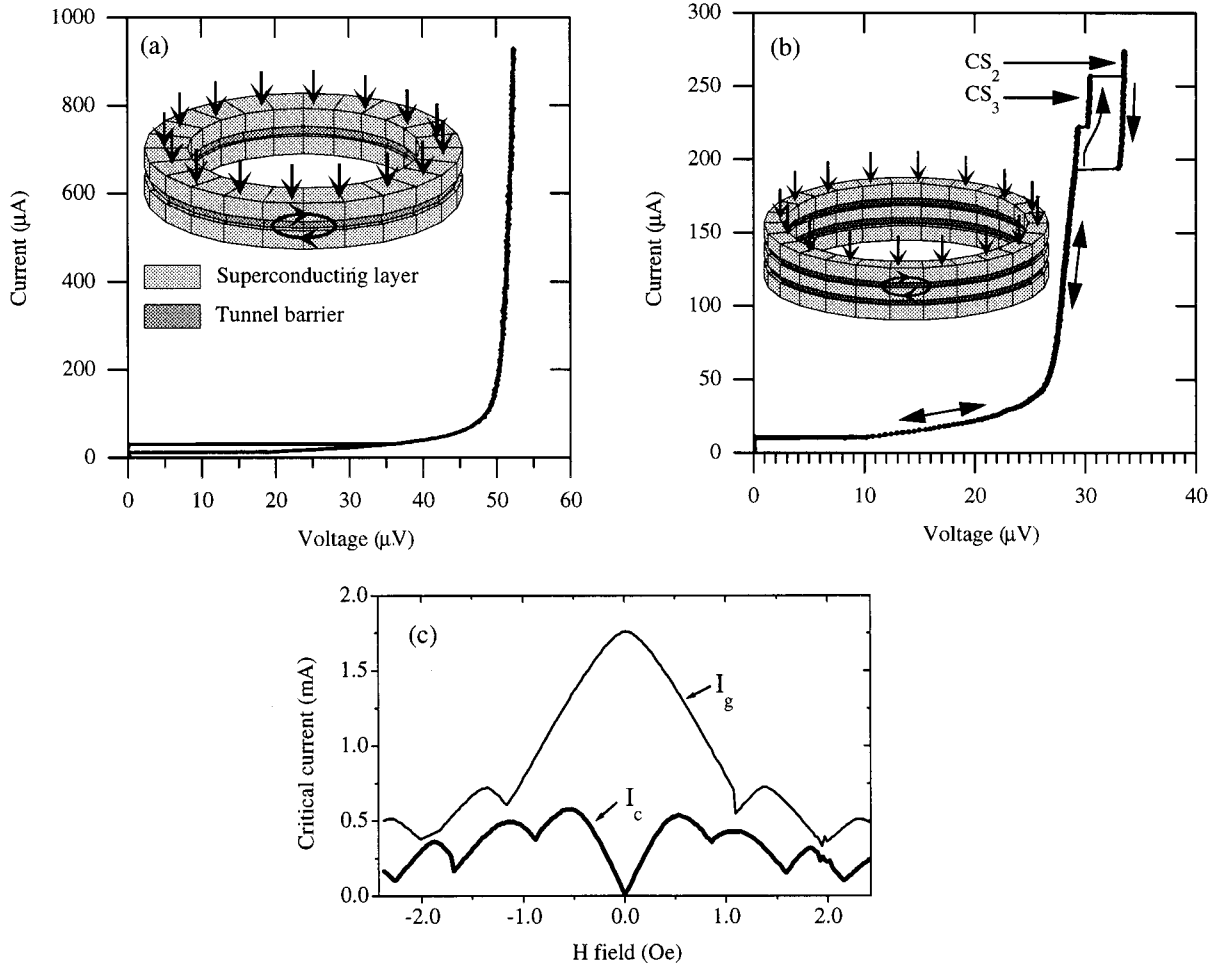


FIG. 1. (a) Current-voltage characteristics (IVC) of a single soliton trapped in a single-layer annular junction. (b) IVC of the double-layer annular junction in the $[1|0]$ soliton configuration. The Cherenkov resonances are marked $CS_{2,3}$. The insets show schematically sample geometries for both cases. (c) $[1|0]$ configuration: Dependence of the critical currents I_c and I_g on magnetic field H applied in the plane of the double-layer junction.

investigation had a ratio of critical current densities j_c^A/j_c^B of about 0.5 (we call junction A the junction with lower j_c), therefore it was easy to distinguish which junction contains soliton.

The soliton step for the $[1|0]$ configuration is shown in Fig. 1(b). The soliton is trapped in the junction A. As compared with Fig. 1(a), we find two additional steps denoted CS_2 and CS_3 (the sense of this notation will be clear later) at voltages $V_{CS_2} \approx 33.3 \mu\text{V}$, and $V_{CS_3} \approx 30.3 \mu\text{V}$. Similar IVC's were observed in several other stacked annular LJJ's.

To find the experimental values for the velocities \bar{c}_+ and \bar{c}_- in the stack, we measured the Fiske step (FS) voltage spacing for both in-phase and out-of-phase modes² by applying a magnetic field in the plane of the sample. Using fields up to 35 Oe we observed two families of FS's at voltages above the single-junction gap voltage. In this case, one junction is biased at the gap voltage state and the excess voltage is generated by cavity resonances in the other junction. We obtained $\Delta V_- \approx 30 \mu\text{V}$ and $\Delta V_+ \approx 56 \mu\text{V}$ for the FS spacing in the out-of-phase and in-phase mode, respectively. From this data the coupling parameter is estimated as

$$S = -\frac{\Delta V_+^2 - \Delta V_-^2}{\Delta V_+^2 + \Delta V_-^2} \approx -0.55$$

and the limiting velocities $\bar{c}_+ \approx 0.038c$, $\bar{c}_- \approx 0.020c$ and $\bar{c}_0 \approx 0.025c$ are calculated. This value of \bar{c}_0 is lower than the one obtained for single uncoupled LJJ due to the smaller thickness of the middle Nb electrode, and it corresponds to the asymptotic voltage $V_1 \approx 37.4 \mu\text{V}$. The steps $CS_{2,3}$ appear at vortex velocities between \bar{c}_- and \bar{c}_0 .

Cherenkov radiation can appear if the soliton velocity u is equal to the phase velocity of emitted linear electromagnetic waves (out-of-phase mode):

$$u = \frac{\omega(k)}{k} = \bar{c}_0 \sqrt{\frac{1}{1-S} + \left(\frac{1}{\lambda_j k}\right)^2}, \quad (1)$$

where ω is the angular frequency of waves and k is their wave number. In the annular LJJ of length L , periodic boundary conditions give the following eigenvalues for k :

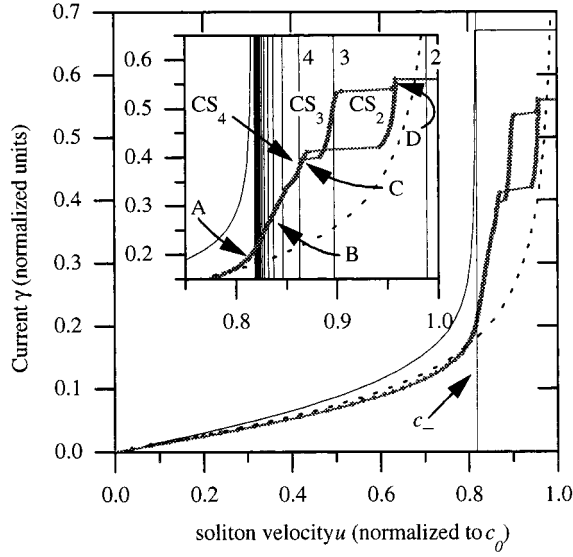


FIG. 2. Calculated dependence of velocity u on bias current density γ (normalized IVC) for one soliton in a two-junction ring for $L/\lambda_J=7$, $\alpha=0.1$, $J=0.5$, $S=-0.5$. The inset shows in detail the top part of the IVC. The IVC for different configurations are shown for comparison: dotted line — single annular junction ($S=0$), thin line — stack in $[1|-1]$ state.

$$k_m = \frac{2\pi}{L}m, \quad \text{where } m=1,2,\dots,\infty. \quad (2)$$

Thus, Cherenkov radiation, if it exists, should lead to resonances at vortex velocities Eq. (1) with k given by Eq. (2):

$$u_m = \frac{\omega(k_m)}{k_m} = \sqrt{c_-^2 + \left(\frac{L}{2\pi\lambda_J m}\right)^2}. \quad (3)$$

To check this idea, the system of two coupled perturbed sine-Gordon equations

$$\begin{aligned} \frac{1}{1-S^2} \phi_{xx}^A - \phi_{tt}^A - \sin\phi^A - \frac{S}{1-S^2} \phi_{xx}^B &= \alpha \phi_t^A - \gamma, \\ \frac{1}{1-S^2} \phi_{xx}^B - \phi_{tt}^B - \frac{1}{J} \sin\phi^B - \frac{S}{1-S^2} \phi_{xx}^A &= \alpha \phi_t^B - \gamma, \end{aligned}$$

that describe the dynamics of the superconducting phase differences $\phi^{A,B}(\tilde{x}, \tilde{t})$ for both LJJ's was solved numerically using periodic boundary conditions. The normalized units for space \tilde{x} and time \tilde{t} as well as the simulation technique are described in detail elsewhere.¹⁰ The simulated IVC of the stack for the $[1|0]$ state is shown in Fig. 2. The choice of parameters $L/\lambda_J=7$ and $S=-0.5$ was close to our experimental values, while the damping constant $\alpha=0.1$ was taken 10 times larger than in the experiment in order to decrease the transient calculation time. The parameter $J=j_c^A/j_c^B=0.5$ is the ratio of the critical current densities. For comparison, the IVCs for $S=0$, and $S=-0.5$ in the $[1|-1]$ state are shown in Fig. 2 by dotted and thin lines, respectively.

First, from simulations we find that for some values of the normalized bias density $\gamma=j/j_c^A$, the soliton velocity u is larger than \bar{c}_- , i.e., \bar{c}_- is not the maximum velocity of the soliton in the $[1|0]$ configuration for $J<1$. Second, there are

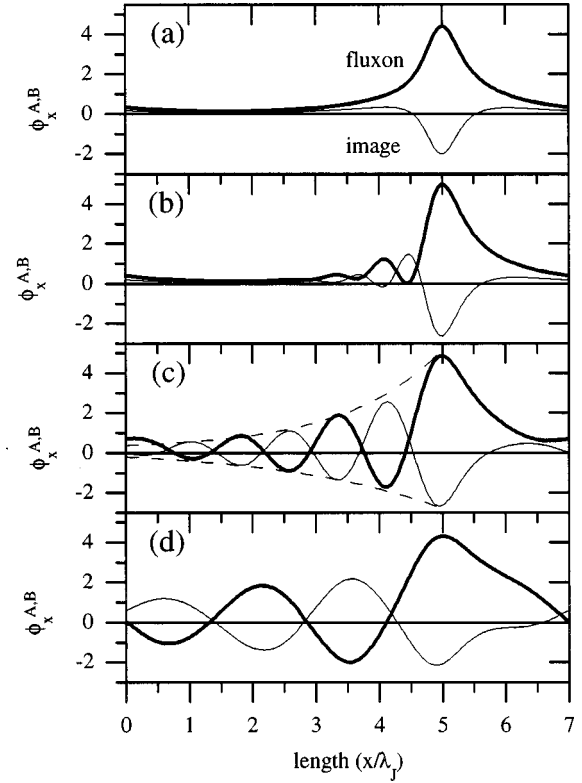


FIG. 3. Profiles of $\phi_x^{A,B}(x)$ in both JJ's. (a), (b), (c), (d) correspond, respectively, to IVC points A, B, C, D shown in the inset of Fig. 2.

two steps to the right from \bar{c}_- which look very similar to the branches $CS_{2,3}$ observed in the experiment. We calculated the phase gradient profiles $\phi_x^{A,B}(\tilde{x})$ for various points of the IVC. If one increases γ from 0 to 1, the soliton dynamics develops in the following way. In the region $0 < u < \bar{c}_-$ the soliton motion is qualitatively well described by the perturbation approach ($|S| \ll 1$) (Ref. 11) and we find the Lorentz contracted soliton in LJJ^A and its image in LJJ^B. Their profiles are shown in Fig. 3(a) and correspond to point A on the IVC (see inset in Fig. 2). As soon as u exceeds \bar{c}_- , an oscillating wake arises behind the moving soliton and its image as shown in Fig. 3(b) which corresponds to point B on the IVC. This wake can be interpreted as Cherenkov radiation. With increasing soliton velocity, the wavelength of the radiation increases in agreement with Eq. (1), and the amplitude and length of the wake grow quickly. The amplitude of the wake decays exponentially in time and space as can be seen from Fig. 3(c) corresponding to point C on the IVC (see inset in Fig. 2). In any point of the IVC the area under the soliton profile is $\int \phi_x^A d\tilde{x} = 2\pi$ and for the image $\int \phi_x^B d\tilde{x} = 0$.

Since the soliton moves in the annular LJJ of finite length L , at some velocity u the Cherenkov radiation wake extends over $\sim L$ so that soliton and its image “see” their own radiation wakes after turning around the junction. This limit is illustrated in Fig. 3(d) and corresponds to point D on the IVC (see the inset of Fig. 2). The interaction of the soliton with its Cherenkov radiation wake results in the appearance of resonances on the IVC of the system at $u > \bar{c}_-$. We call these resonances “Cherenkov steps”. On resonance the

oscillations of $\phi^{A,B}$ in the JJ's induced by the moving soliton take place in phase (show constructive interference) with Cherenkov-generated Josephson plasma waves $\phi^{A,B}$ [Fig. 3(d)]. Thus, the experimentally observed steps CS_{2,3} on the IVC in Fig. 1 can be ascribed to the interference between the moving soliton and its Cherenkov radiation.

The resonant velocities calculated using Eq. (3) are shown in Fig. 2 by thin vertical lines with m indicated by numbers. One can see that the simple formula (3) fairly well describes the positions of the resonances obtained in simulations for $m > 2$. For example, Fig. 3(c) with the $m=4$ cavity mode corresponds to the resonant step located at the voltage close to $u=u_4$. The deviation of the resonance CS₂ from (3) can be explained by strong nonlinearity of high amplitude waves behind the soliton for small m [see Fig. 3(d)] which is not taken into account by our model for small-amplitude linear waves. The density of the resonances increases with m up to infinity when $u \rightarrow \bar{c}_- + 0$. Since the resonances have a finite width due to damping, it is possible to resolve only the CS's with not very large m in JJ's of moderate length L/λ_J . Our numerical study showed that for $\alpha=0.1$ individual resonances appear up to $L/\lambda_J \sim 30$.

Using the experimentally obtained velocity \bar{c}_- and coupling constant S , we can calculate the Cherenkov resonance numbers m that correspond to CS_{2,3} in Fig. 1(b). Using Eq. (3) with experimentally estimated normalized length $L/\lambda_J=7$, the best correspondence can be obtained for $m=2$ and 3 (now, the sense of notations CS_{2,3} is clear). The calculated CS's voltages are $V_{CS_2}=36.6 \mu\text{V}$, and $V_{CS_3}=33.2 \mu\text{V}$. These voltages are in rather good agreement with experiment. However, the agreement is not ex-

pected to be perfect due to the very low damping $\alpha \sim 0.01$ in our LJJ's. Therefore, the Cherenkov radiation consists of high amplitude plasma waves so that some discrepancy with the small amplitude model (3) is expected. When choosing the values of m we tried to satisfy two criteria. First, according to our simulations, the steps calculated using Eq. (3) should have somewhat higher voltages than in the real system. Second, as pointed out above, the linear wave approximation works better for higher m , so that, $V_{CS_m}^{\text{theor}} - V_{CS_m}^{\text{exp}}$ should decrease with m . Both conditions are satisfied with the above choice of m .

In this paper we considered stacks with equal Swihart velocities of junctions $\bar{c}_0^A = \bar{c}_0^B$. If $\bar{c}_0^A \neq \bar{c}_0^B$, Cherenkov radiation also takes place for $u > \bar{c}_-$. In the case of weak coupling $|S| \ll 1$ the limiting velocity is $\bar{c}_- \approx \min(\bar{c}_0^A, \bar{c}_0^B)$, and, thus, we obtain the condition for Cherenkov radiation from the earlier theoretical work:¹¹ At $|S| \ll 1$ the Cherenkov emission takes place at $u > \bar{c}_0^B$ for a soliton moving in LJJ^A if $\bar{c}_0^A > \bar{c}_0^B$.

Despite earlier theoretical predictions,^{11,12} to our knowledge, Cherenkov radiation was not observed in any Josephson system before this work. From the physical picture of the effect presented in this paper, we also conclude that Cherenkov radiation from fast moving Josephson vortices should also take place in intrinsic stacks of LJJ's, i.e., in naturally layered high- T_c superconductors such as Ba₂Sr₂CaCu₂O_{8-x}.

We would like to thank G. Hechtfisher, N. F. Pedersen, and S. Sakai for useful discussions.

*Also at Inst. of Radio Eng. and Electronics, Moscow, 103907, Russia. Electronic mail: goldobin@mars.isi.kfa-juelich.de

†Also at Physikalisches Institut III, Universität Erlangen-Nürnberg, D-91058, Erlangen, Germany.

¹S. Sakai, P. Bodin, and N. F. Pedersen, J. Appl. Phys. **73**, 2411 (1993).

²A. V. Ustinov, H. Kohlstedt, M. Cirillo, N. F. Pedersen, G. Hallmanns, and C. Heiden, Phys. Rev. B **48**, 10 614 (1993).

³N. Grønbech-Jensen, D. Cai, and M. R. Samuelsen, Phys. Rev. B **48**, 16 160 (1993).

⁴R. Kleiner, F. Steinmeyer, G. Kunkel, and P. Müller, Phys. Rev. Lett. **68**, 2394 (1992); R. Kleiner and P. Müller, Phys. Rev. B **49**, 1327 (1994).

⁵S. Sakai, A. V. Ustinov, H. Kohlstedt, A. Petraglia, and N. F.

Pedersen, Phys. Rev. B **50**, 12 905 (1994).

⁶R. Kleiner, Phys. Rev. B **50**, 6919 (1994).

⁷A. Davidson, B. Dueholm, B. Kryger, and N. F. Pedersen, Phys. Rev. Lett. **55**, 2059 (1985).

⁸A. V. Ustinov, T. Doderer, R. P. Huebener, N. F. Pedersen, B. Mayer, and V. A. Oboznov, Phys. Rev. Lett. **69**, 1815 (1992).

⁹S. Keil, I. V. Vernik, T. Doderer, A. Laub, H. Preßler, R. P. Huebener, N. Thyssen, A. V. Ustinov, and H. Kohlstedt, Phys. Rev. B **54**, 14 948 (1996).

¹⁰A. Wallraff, E. Goldobin, and A. V. Ustinov, J. Appl. Phys. **80**, 6523 (1996).

¹¹Yu. S. Kivshar and B. A. Malomed, Phys. Rev. B **37**, 9325 (1988); Rev. Mod. Phys. **61**, 763 (1989).

¹²R. G. Mints and I. B. Snapiro, Phys. Rev. B **52**, 9691 (1995).